Effect of Surface Curvature on Critical Adsorption

Rami A. Omari, Christopher A. Grabowski, and Ashis Mukhopadhyay

Department of Physics and Astronomy, Wayne State University, Detroit, Michigan 48201, USA

(Received 12 August 2009; revised manuscript received 21 October 2009; published 25 November 2009)

We studied critical adsorption on curved surfaces by utilizing spherical nanoparticles immersed in a critical binary liquid mixture of 2,6 lutidine + water. The temperature dependence of the adsorbed film thickness and excess adsorption was determined from fluorescence correlation spectroscopy measurements of the enlarged effective hydrodynamic radius of the particles. Our results indicated that the adsorbed film thickness is of the order of correlation length associated with concentration fluctuations. The excess adsorption per unit area increases following a power law in reduced temperature with an exponent of -1, which is the mean-field value for the bulk susceptibility exponent. This has been confirmed with silica particles of two different radii, 10 and 25 nm. The results were also compared with the theoretical mean-field scaling function.

DOI: 10.1103/PhysRevLett.103.225705 PACS numbers: 64.60.F−, 68.08.Bc, 68.18.Fg, 68.35.Rh

In many naturally occurring situations, an extended surface, simple particle or polymer is immersed in a complex fluid environment consisting of multiple components. The local composition of fluids near such entities can be significantly different compared to the bulk due to the preferential adsorption of a solvent component [1]. The width of this preferential adsorption layer is of the order of the solvent correlation length, which is typically a few angstroms, and affects only a few layers of liquid molecules next to the bodies. However, near the critical point, the enhanced adsorption of the preferred component becomes particularly pronounced due to the divergence of correlation length (ξ) associated with critical composition fluctuations [2–5]. Critical adsorption at planar liquid-vapor and liquid-solid surfaces has been extensively studied [4,6–10]. In the limit of strong adsorption, the preferred component completely saturates the surface and surface composition is described by a universal surface scaling function $P(z/\xi)$, where z is the depth away from the surface. It is difficult to measure the universal function directly, and most experimental techniques probe integrals over the adsorption profile. A quantity quite often measured is excess adsorption (Γ), which describes the total enrichment of the preferred component of the fluid. Near the critical temperature (T_c) the excess adsorption diverges as $\Gamma \sim t^{\beta-\nu}$, where t is the reduced temperature $t = |T - T_c|/T_c$ and $\beta \approx 0.33$ and $\nu \approx 0.63$ are the bulk critical exponents associated with the coexistence curve and the correlation length, respectively. Good agreement with theoretical predictions has been obtained for critical adsorption at planar surfaces [4]. However, very little is known about the critical adsorption on a curved substrate, where the effect of surface curvature introduces rich physics into the problem. For spherical particles, the local fluid composition near the surface depends upon two dimensionless variables, $x = z/\xi$ and $y = R_0/\xi$, where R_0 is the radius of the dissolved sphere [3]. Theoretical results have suggested that for a curved surface, the order parameter profile is characterized by a universal surface scaling function $P(z/\xi, R_0/\xi)$. The excess adsorption (Γ) can be obtained from $P(x, y)$ by integrating over $x = z/\xi$, which is also characterized by universal scaling function $G(R_0/\xi)$. Γ is expected to follow a scaling relation, $\Gamma(t \to 0) \sim t^{-\gamma}$, where γ is the bulk susceptibility critical exponent [3]. Verification of these universal functions and scaling relations has proven to be particularly challenging due to lack of experimental methods with the required sensitivity and specificity. This is the first experimental study, to the best of our knowledge, which directly tests the theoretical predictions for critical adsorption on curved objects. The novelty of this investigation is the use of an ultralow concentration of particles, which perturbs the critical behavior of the system minimally and allows determination of adsorption profiles at the surface of a *single* sphere near T_c. The results presented in this Letter will be directly relevant in the areas of surface critical phenomena, colloidal suspensions, and for many soft materials systems (e.g., colloid-polymer mixtures) where there is coupling between two macroscopic length scales. In the broader context, this will aid in understanding the interaction of liquids with surfaces possessing geometric structure [11], the phase behavior of multicomponent fluids [12,13], and wetting phenomena [14–16].

A part of the motivation for this study came from prior observations of thermally induced reversible flocculation phenomena in binary liquid mixtures (2,6 lutidine + water (LW), isobutyric acid + water, etc.) containing a small volume fraction of silica or polystyrene colloidal particles [14,17–19]. The precise interpretation of these experiments still remains somewhat controversial [20–22]. The colloidal particles used in many of these experiments possess surface negative charges. If one component in the mixture preferentially adsorbs onto the particles, an adsorbed film of the phase rich in that component can

develop onto them. As the phase separation temperature of the liquid mixture is approached, the thickness of the adsorbed layer around the colloidal particles increases. The presence of such films can induce long-ranged attractive forces between particles, which could lead to flocculation in these systems [14,20]. Alternatively, flocculation may be linked to a phase separation in the ternary mixture when a high concentration of particles is used [12]. If the liquid mixture is near the critical point, the interference of critical adsorption profiles on neighboring particles can give rise to an attractive critical Casimir force [23]. This has also been argued to contribute to flocculation for a near-critical solvent mixture [24–26]. To properly assess the role of the critical Casimir force on aggregation phenomena, the knowledge of the adsorption profile at the surface of a single sphere near T_c will be highly desirable. We achieve this goal by using the single-molecule sensitive technique of fluorescence correlation spectroscopy (FCS), which measured the ''enlarged effective hydrodynamic radius'' (R) of the particles due to critical adsorption.

The choice of this particular method was guided by several of its advantages. The particle volume fraction in these experiments is much lower ($<10^{-5}$ v/v) compared to other traditional methods of particle-size measurements, such as scattering. In this situation, the particles can be regarded as isolated because their average spacing would be greater than a few microns, which is much larger than their size or Debye length ($\approx$20 nm). The low concentration of particles does not alter the critical behaviors, such as the critical temperature and critical composition as was verified by performing control experiments. In addition, the critical opalescence of the solution near T_c poses less of a significant problem due to specificity of this method [27]. Experiments were performed with fluorescently labeled green silica nanospheres (Microspheres-Nanospheres, Inc.) of radii approximately 25 and 10 nm. The critical mixture used was 2,6 lutidine + water. LW has an inverted coexistence curve with a lower critical temperature of $\sim$33.9 °C and the critical composition of 28.2% lutidine by weight. These particles possess a small surface charge, so that lutidine preferentially adsorbs onto the surface of the particles. This was verified by observing that the majority of the particles reside in the lutidine-rich phase in the two-phase region. By using a commercial temperature controller (Lakeshore, Inc.) and a homebuilt sample cell, the temperature is regulated $\pm$3 mK over 1 h. By taking measurements within 25 mK of T_c, the experiments have allowed us to vary the size ratio by a factor of about 30.

The setup used was as described earlier. Briefly, the sample cell was placed on the stage of a Zeiss inverted microscope. Near-infrared light from a femtosecond Ti:sapphire laser (800 nm, 80 MHz, pulse width $\sim$100 fsec) was focused through a long working distance objective (63 ×, NA = 0.75) into the sample. Fluorescence was collected through the same objective and detected by single photon counting modules (Hamamatsu). The laser power was kept below 1 mW. Two-photon excitation of the fluorophores at the diffraction-limited focus of a laser beam allowed us to measure diffusion within a tiny focal volume of the order of 0.1 fl [Fig. 1(a)]. The small number of particles contained within a given volume fluctuates as the labeled nanoparticles diffuse into and out of the laser focus [Fig. 1(b)]. By calculating the autocorrelation function $C(\tau)$ of this fluctuation (F), $C(\tau) = \langle \delta F(t) \delta F(t+\tau) \rangle / \langle F(t) \rangle^2$, and using a suitable model to analyze it, the center-of-mass diffusion coefficient (D) of the particles is obtained. The hydrodynamic radius (R) of the particle is determined from the measured diffusion coefficient by using the Stokes-Einstein (SE) relation: $R = k_B T / 6\pi\eta D$, where k_B is Boltzmann's constant, T is the absolute temperature, and η is the viscosity of the binary solvent [Fig. 1(c) inset]. All experiments were performed at the one-phase region of the liquid mixture.

Figure 1(c) shows autocorrelation functions collected during this experiment at two different temperatures for particles of radius $R_0 \approx 25$ nm. We used a model of Fickian diffusion process in three dimensions, $C(\tau) = C(0)/[(1 + 8D\tau/\omega_0^2)\sqrt{(1 + 8D\tau/z_0^2)}]$ to analyze the curves. In this relation, ω_0 and z_0 are the dimensions of the excitation focus in lateral and axial directions, respectively. They were determined by a calibration experiment using fluorescein both in water as well as using LW mixture. The fitting of the autocorrelation function (ACF) gives values for the diffusion coefficient (D). Far away from T_c, by averaging over 3–4 measurements, we determined $D \approx 3.5$ μm^2/s and 8 μm^2/s in LW critical mix-

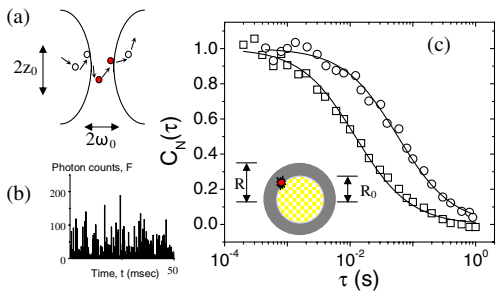

FIG. 1 (color online). Experimental scheme. (a) A focused femtosecond laser caused two-photon excitation of fluorophores within a cylindrical volume of dimensions $\omega_0 \sim 0.4$ μm and $z_0 \sim 2$ μm. (b) Photon emission counts fluctuate with time, resulting from diffusion of particles into and out of the focus spot. (c) Normalized intensity-intensity autocorrelation functions $C_N(\tau)$ of $R_0 \approx 25$ nm SiO_2 colloids plotted as a function of logarithmic time lag τ for two temperatures: $\Delta T = T_c - T = 1.125$ K (squares, $D = 3.56$ μm^2/s) and $\Delta T = 0.025$ K (circles, $D = 0.88$ μm^2/s). The solid lines correspond to single diffusion time fits. Inset: The schematic of a nanoparticle attached with a fluorescent dye and an adsorbed liquid layer. R_0 is the radius of the solid core and $R - R_0$ is the thickness of the adsorbed film.

ture for $R_0 = 25$ and 10 nm particles, respectively. These are close to the expectation from SE relation based upon the known viscosity of the solution ($\eta = 2.6$ cP) at room temperature [28]. In addition, the ACFs can be fitted with a single diffusion coefficient indicating that the polydispersity of the particles can be neglected.

Figure 2 shows the variation of diffusion coefficients for both particles as a function of ΔT ($=T_c - T$), which decreases as the critical temperature is approached. This trend is reproducible with different samples, and we have verified that it is not an artifact from the turbidity of the mixture close to T_c. By taking into account the temperature dependence of viscosity and, in particular, its weak divergence near T_c, we have determined the hydrodynamic radius (R) [28]. By subtracting the core size of the particle (R_0), the thickness of the adsorbed layer has been obtained, which was plotted against the reduced temperature (t) in the Fig. 2 insets. The data indicate an enhancement of the adsorbed film thickness as the T_c is approached. Please note the caveat we have used here. The ''radius'' that has

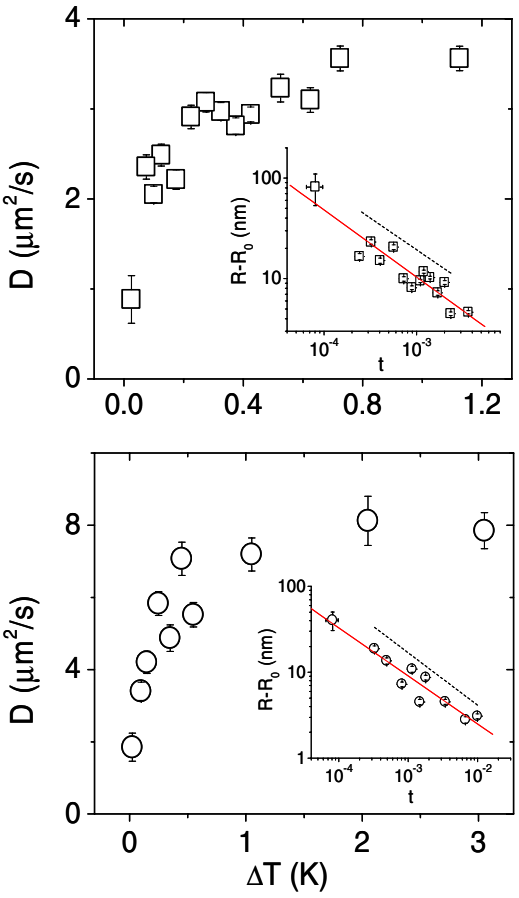

FIG. 2 (color online). Diffusion coefficient of 25 nm (top) and 10 nm (bottom) SiO_2 particles plotted against ΔT. Insets: The thickness of the adsorbed liquid layer on the surface of particles plotted as a function of reduced temperature (t). The solid line is the best fit and the dashed line is the variation of the correlation length (ξ).

been determined in these experiments is a phenomenological parameter because particles with adsorbed liquid layer can no longer be considered as a solid sphere. The frictional drag of the adsorbed layer when it is moving through the bulk liquid is difficult to estimate [19]. It has also been argued that near the critical point, when the growing correlation length becomes larger than the particle size, the SE relation could break down [29]. However, we have verified through studies of diffusion of fluorescent molecules that SE relation is obeyed even very close to T_c [27]. Within the temperature range investigated, the thickness of the adsorbed film follows a behavior similar to the t dependence of correlation length, which is given by $\xi = \xi_0 t^{-\nu}$. The nonuniversal correlation length amplitude (ξ_0) is ≈ 0.25 nm in the one-phase region of the binary solvent [2]. The best fit of the data in Fig. 2 (inset) shows, $R - R_0 = 0.1t^{-0.66}$ nm for 25 nm particles and $R - R_0 = 0.19t^{-0.56}$ nm for 10 nm particles. Even for particles with large adsorbed films, as observed very close to T_c, their average separation is much higher so that no perturbation to the adsorption profile is expected from their overlap.

The excess adsorption (Γ), which describes the total enrichment of the preferred component by volume, has been determined by using the relation $\Gamma = 4\pi(R^3 - R_0^3)/3$. This is based upon the assumption that the local order parameter decays in steplike manner at a distance R from the center of the particle. We define a dimensionless quantity Γ_e where $\Gamma_e = \Gamma/(A_0 M_- \xi_0)$; $A_0 = 4\pi R_0^2$ is the surface area of the particle, and M_- is the coefficient of the bulk order parameter, which is ≈ 0.9 for LW [2]. The currently available theoretical studies indicate that Γ_e is governed by a universal scaling function, which in the limit $t \to 0$ is given by $\Gamma_e(y) = g_+[(t^{\beta-\nu} - 1)/(\nu - \beta)] + t^{\beta-\nu} G(y)$ [3]. Here, g_+ is a universal number, whose numerical value ≈ 0.6, $y = R_0/\xi$ is the size ratio, β and ν are the critical exponents associated with order parameter and composition fluctuations, respectively [2]. Within mean-field approximation, $\Gamma_e(y) = g_+|\ln|t|| + G(y)$. To compare the experimental results directly with the scaling function $G(y)$, in Fig. 3 we plotted $G_{\rm exp} = \{\Gamma_e - g_+[(t^{\beta-\nu} - 1)/(\nu - \beta)]\}t^{\nu-\beta}$ as a function of y by using Ising exponents, $\beta \approx 0.32$, $\nu \approx 0.63$. The results for the two different sized particles indicate that although their functional forms are similar, the excess adsorption for $R_0 \approx 10$ nm particles is systematically lower compared to the bigger particles. There is admittedly some uncertainty in determining R_0, which can affect both Γ_e and y. More specifically, for the bigger particle, dynamic light scattering (DLS) yielded a higher value for R_0 (≈ 31 nm) compared to transmission electron microscopy (TEM) experiments, which gives $R_0 \approx 24$ nm. Such differences in results between DLS and TEM measurements have been noted previously [30]. FCS experiments performed at a temperature far below T_c ($\Delta T > 10\,^\circ$C) measured $R_0 \approx 26$ nm. We fixed R_0 at the value we obtained from FCS

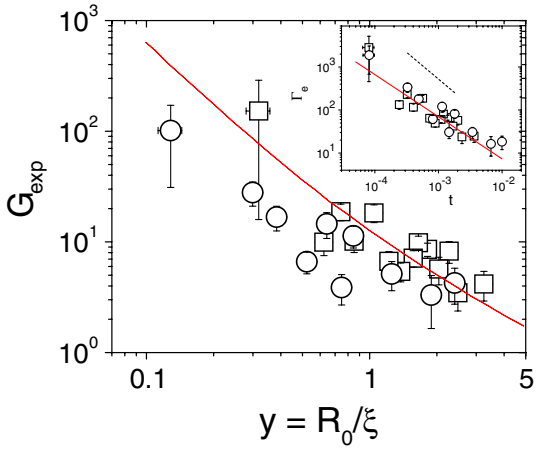

FIG. 3 (color online). The quantity G_{exp} plotted as a function of $y = R_0/\xi$ for both particles (squares, 25 nm; circles, 10 nm). The solid line is the theoretical mean-field prediction. Inset: Γ_e vs t on a log-log scale. The solid line through the data corresponds to slope of -0.98. The dashed line has a slope of -1.24.

measurements taken far away from T_c to obtain excess adsorption and the adsorbed layer thickness. The relative standard deviation over several measurements is about 5%. Theoretically, the full functional form for $G(y)$ is available only within the mean-field approximation [3], which is plotted in Fig. 3. The functional form of the theoretical prediction for excess adsorption matches well with the experimental data. The quantitative difference between them might originate from the simplistic assumption that the friction coefficient of a ''liquid ball with a solid core'' is still given by the Stokes equation, $f = 6\pi\eta R$. This, in turn, can affect determination of excess adsorption because of its cubic dependence on R. Good data collapse is obtained when Γ_e is plotted versus reduced temperature as shown in the Fig. 3 inset. The solid line is a least squares fit of the data to a power law. The slope of this line is -0.98 ± 0.09, which is close to the mean-field value of the bulk susceptibility exponent (γ). For comparison we have also plotted in the figure the expectation from the Ising exponent. A future goal is to extend these measurements even closer to T_c to test whether the Ising exponent for γ is recovered. This is not yet possible because of the difficulty of combining single-molecule sensitive spectroscopy technique with a sample cell that provides better than a mK temperature stability.

In summary, we have introduced a novel experimental method to study the critical adsorption on particles possessing high surface curvature. Using it, we have determined the temperature dependence of the adsorbed film thickness and excess adsorption near the critical point of a binary liquid mixture. The results from this investigation will be relevant in understanding the collective behavior of colloidal suspensions and in situations where fluids interact with structured substrates such as in microfluidic devices.

We thank Professor Mike Solomon and Professor David Oupicky for help with DLS and zeta potential measurements. Acknowledgements are made to the American Chemical Society Petroleum Research fund (PRF No. 44953-G5), and to the National Science Foundation through Grant No. DMR-0605900 for support of this research.

[1] M. E. Fisher and P. G. de Gennes, C.R. Seances Acad. Sci., Ser. B **287**, 207 (1978).
[2] D. S. P. Smith *et al.*, Phys. Rev. E **55**, 620 (1997).
[3] A. Hanke and S. Dietrich, Phys. Rev. E **59**, 5081 (1999).
[4] B. M. Law *et al.*, Eur. Phys. J. Special Topics **167**, 127 (2009).
[5] S. Gnutzmann and U. Ritschel, Z. Phys. B **96**, 391 (1995).
[6] R. Garcia *et al.*, Phys. Rev. E **68**, 056111 (2003).
[7] H. W. Diehl and M. Smock, Phys. Rev. B **47**, 5841 (1993).
[8] G. Flöter and S. Dietrich, Z. Phys. B **97**, 213 (1995).
[9] H. Zhao *et al.*, Phys. Rev. Lett. **75**, 1977 (1995).
[10] J. Jestin *et al.*, Eur. Phys. J. B **24**, 541 (2001).
[11] C. RascÓn and A. O. Parry, Nature (London) **407**, 986 (2000).
[12] Y. Jayalakshmi and E. W. Kaler, Phys. Rev. Lett. **78**, 1379 (1997).
[13] H. Guo *et al.*, Phys. Rev. Lett. **100**, 188303 (2008).
[14] D. Beysens and T. Narayanan, J. Stat. Phys. **95**, 997 (1999).
[15] M. C. Stewart and R. Evans, Phys. Rev. E **71**, 011602 (2005).
[16] D. Bonn *et al.*, Rev. Mod. Phys. **81**, 739 (2009).
[17] D. Beysens and D. Estève, Phys. Rev. Lett. **54**, 2123 (1985).
[18] V. Gurfein, D. Beysens, and F. Perrot, Phys. Rev. A **40**, 2543 (1989).
[19] P. D. Gallagher, M. L. Kurnaz, and J. V. Maher, Phys. Rev. A **46**, 7750 (1992).
[20] B. M. Law, J.-M. Petit, and D. Beysens, Phys. Rev. E **57**, 5782 (1998).
[21] R. R. Netz, Phys. Rev. Lett. **76**, 3646 (1996).
[22] T. J. Sluckin, Phys. Rev. A **41**, 960 (1990).
[23] C. Hertlein *et al.*, Nature (London) **451**, 172 (2008).
[24] F. Schlesener, A. Hanke, and S. Dietrich, J. Stat. Phys. **110**, 981 (2003).
[25] T. W. Burkhardt and E. Eisenriegler, Phys. Rev. Lett. **74**, 3189 (1995).
[26] A. Hanke *et al.*, Phys. Rev. Lett. **81**, 1885 (1998).
[27] C. Grabowski and A. Mukhopadhyay, Phys. Rev. Lett. **98**, 207801 (2007).
[28] E. Gülari *et al.*, J. Chem. Phys. **56**, 6169 (1972).
[29] G. Biroli and J. P. Bouchaud, J. Phys. Condens. Matter **19**, 205101 (2007).
[30] J. C. Thomas, J. Colloid Interface Sci. **117**, 187 (1987).